THE QPOS AWAKEN IN THE QUEST FOR PULSATING ULXS

MATTEO IMBROGNO

Collaborators:
Gian Luca Israel,
Roberta Amato,
Guillermo Andres
Rodríguez Castillo,
Sara Motta,
Felix Fuerst,
and many others

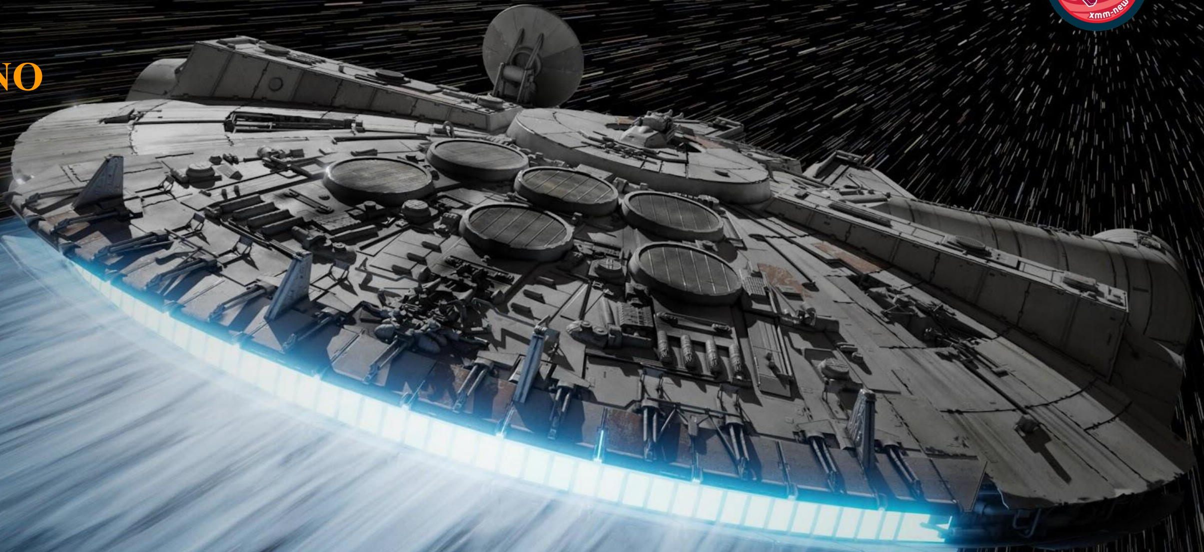

XMM-NEWTON
WORKSHOP
5/6/2024

TOR VERGATA
UNIVERSITÀ DEGLI STUDI DI ROMA

STVDIVM VRBIS

INAF
ISTITUTO NAZIONALE
DI ASTROFISICA

QUASI-PERIODIC OSCILLATIONS

Motta+ 2011

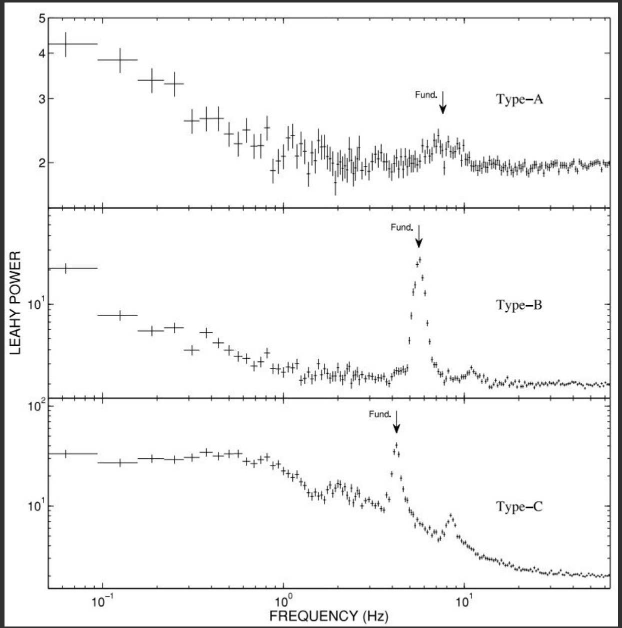

Smith+ 2018

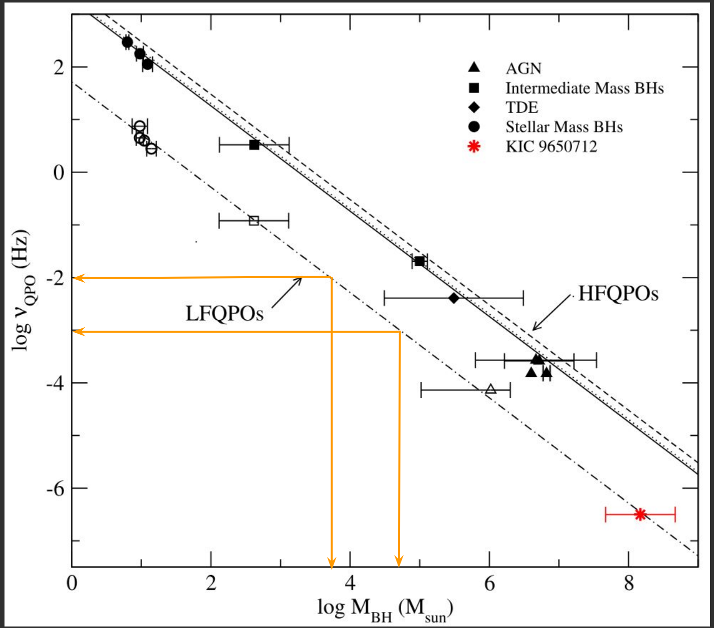

- QPOs: broad features in the PDS.
- **Quality factor**: $Q = \nu/\Delta\nu > 2$.
- Related to **instabilities in the disk** and/or **precession of the disk**.

- Relation between the frequency ν and the mass M_{BH} of the accretor.
- Lower ν ⟶ higher mass.

QPO IN ULXS

- Atapin+ 2019: sample of 5 ULXs for which QPOs have been detected.
- Strohmayer+ 2007, 2009: mHz QPO in M82 X-1 and NGC 5408 X-1.
- **Early 2000's: we finally found the IMBHs, right?**

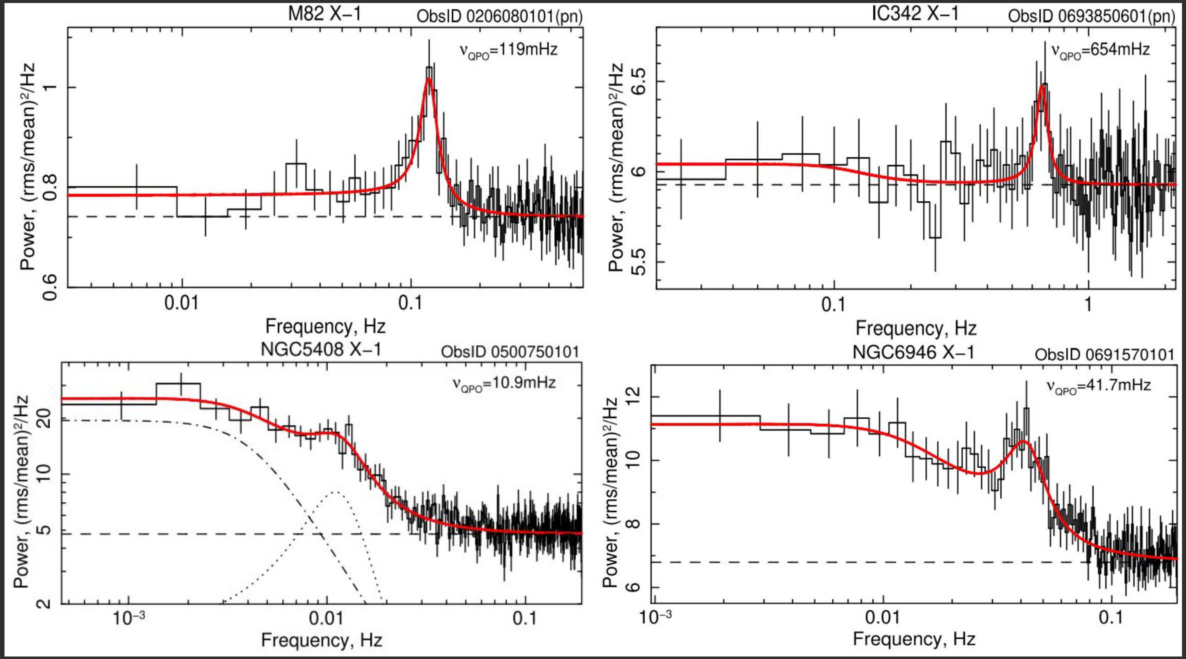

M82 X-2: AN INTERMEDIATE MASS... NO, THE FIRST PULX

Feng+ 2010

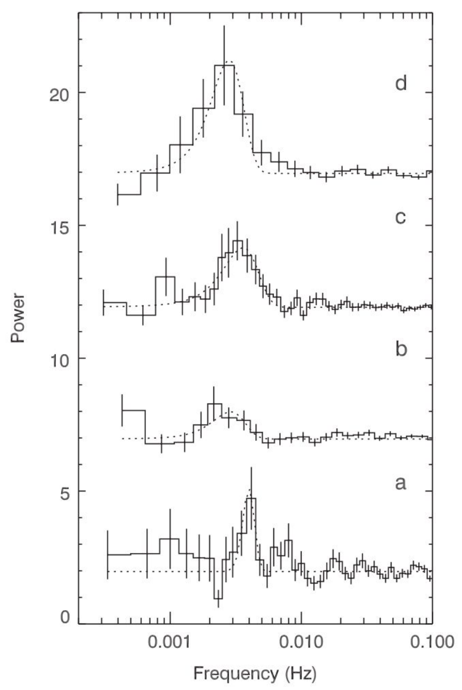

- Feng+ 2010: QPOs at $\nu \simeq$ 3-4 mHz in M82 X-2 (X42.3+59 in their work).
- Scaling the mass with the frequency:
  $M_{source} \sim 12000 - 43000\ M_{\odot}$
  A new IMBH?
- Bachetti+ 2014: discovery of spin pulsations at a period $P \simeq 1.3$ s.

↓

It must be a neutron star: the first PULX!

Bachetti+ 2014

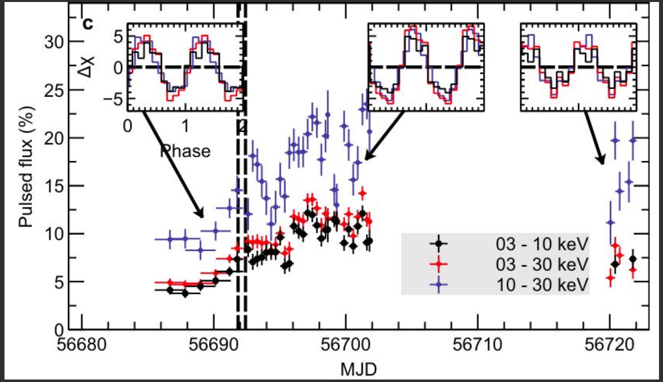

M51 ULX-7: THE DISCOVERY OF THE SPIN PULSATION

- Signal identified through **accelerated search techniques** in 2018 XMM observations.

- **Variable PF** (~ 5 - 20%), even within the same obs.

- Source parameters:
  - P_{spin} ~ 2.8 s
  - P_{orb} ~ 2 d
  - $a_x \sin i$ ~ 28 lt-s
  - $\dot{P}$ ~ -10^{-10} s s^{-1}
  - $\dot{P}_{sec}$ ~ -10^{-9} s s^{-1}

Castillo+ 2020

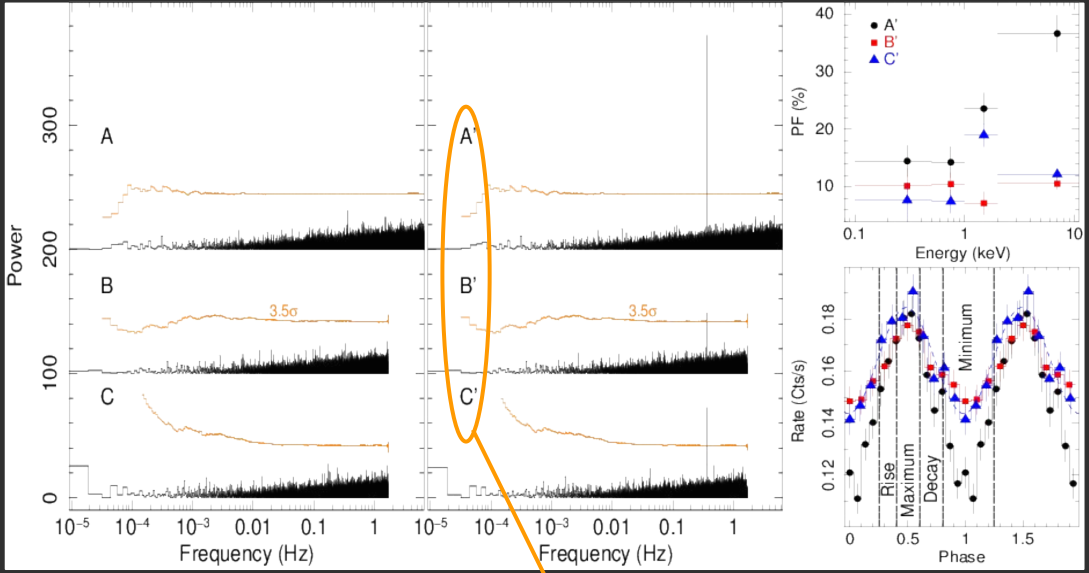

PDSs after the $\dot{P}$ and orbital Doppler correction.

GET TO KNOW ULX-7 A BIT MORE

Brightman+ 2022

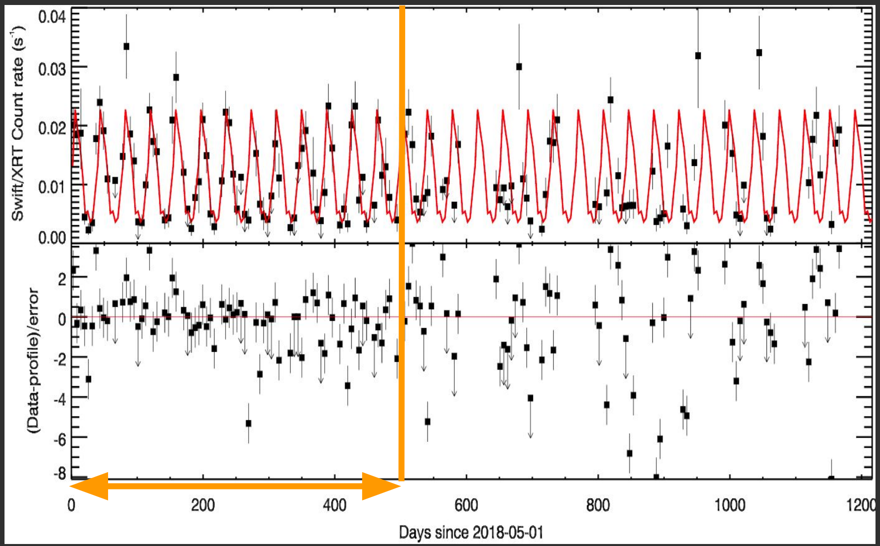

Castillo+ 2020

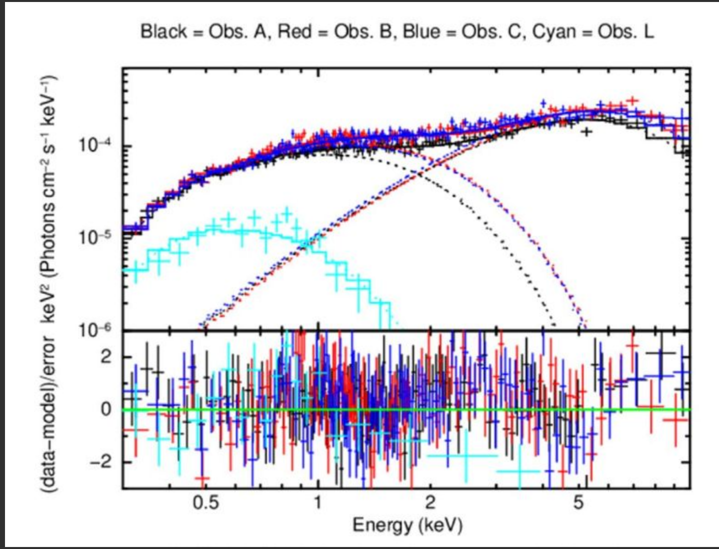

- **Superorbital modulation**: Brightman+ 2020 (P ≃ 38 d), **signs of evolution** towards P ≃ 44 d (Brightman+ 2022).
- Peak luminosity: $L_X \simeq (5\text{-}7) \times 10^{39}$ erg s^{-1}

- Persistent source (detected in 13 out of 14 XMM observations).
- 2018: Pulsation detected when the hard component is visible.

ULX-7: THE DISCOVERY OF THE QPO

Imbrogno+, submitted

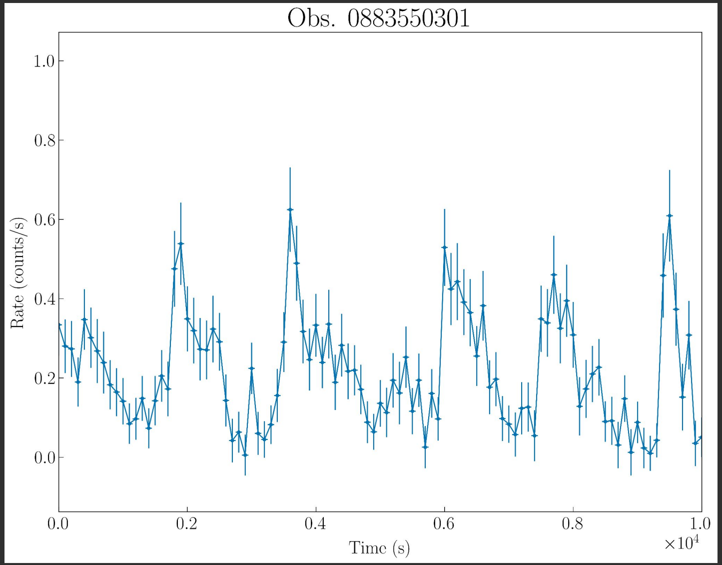

Imbrogno+, submitted

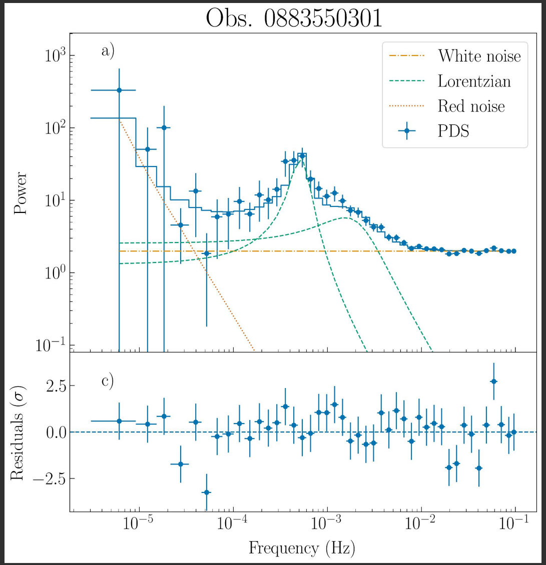

- 3 XMM obs in 2021/2022: **recurring, ks-long flaring feature in the light curve**.
- Absent in 2018 observations.

- Broad component (Q < 2) at 1 mHz. QPO (Q > 2) at 0.5 mHz.
- No coherent signal at 2.8 s, PF 3σ upper limit at 6%: **absence caused by this feature**?

ULX-7: SPECTRAL ANALYSIS

- Model: two multi-temperature disk black bodies. Two absorption component (MW+local).
- Consistent with Castillo+ 2020: **no change in spectral state**.
- $L_X \simeq 5 \times 10^{39}$ erg s^{-1}

Imbrogno+, submitted

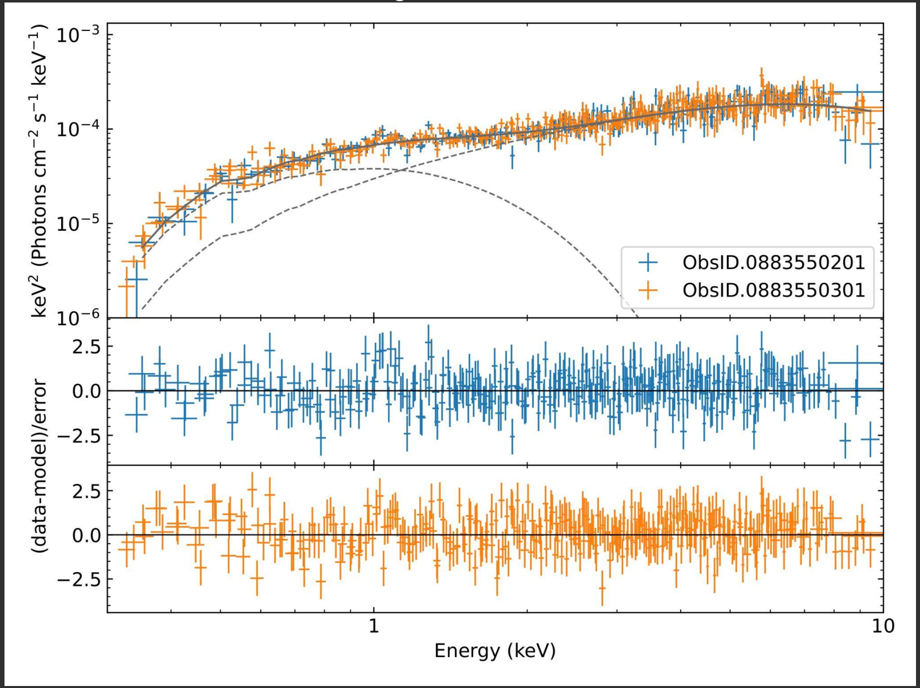

ULX-7: ARCHIVAL DATA AND POSSIBLE EXPLANATIONS

- Feature detected in 5 consecutive Chandra archival observations.
  Little variability between the two epochs (10 years apart).

- QPO detected at super-Eddington luminosities, like M82 X-2.
  Never present in XMM observations in which the pulsation is detected.

- Our hypothesis: **the QPO is decreasing the pulsed fraction of the spin signal**.

- Middleton+ 2019: **Lense-Thirring precession, QPO arising from precessing winds**.
  Problem: B $\ll 10^9$ G required. Or maybe not (but beware of fine tuning)…

Imbrogno+, submitted

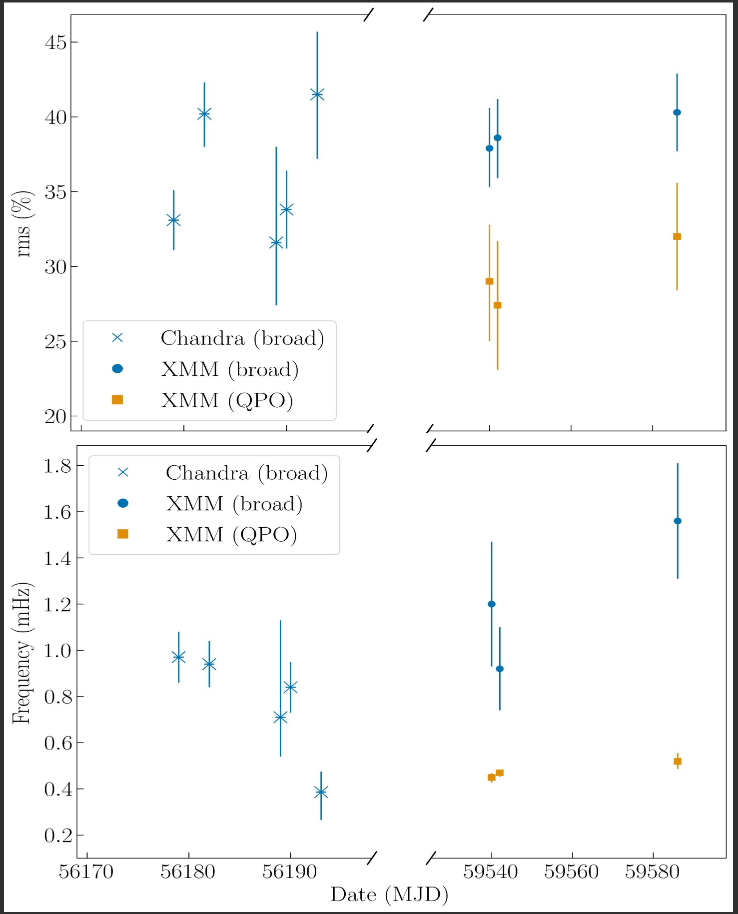

NGC 7793 P13

Israel+ 2017

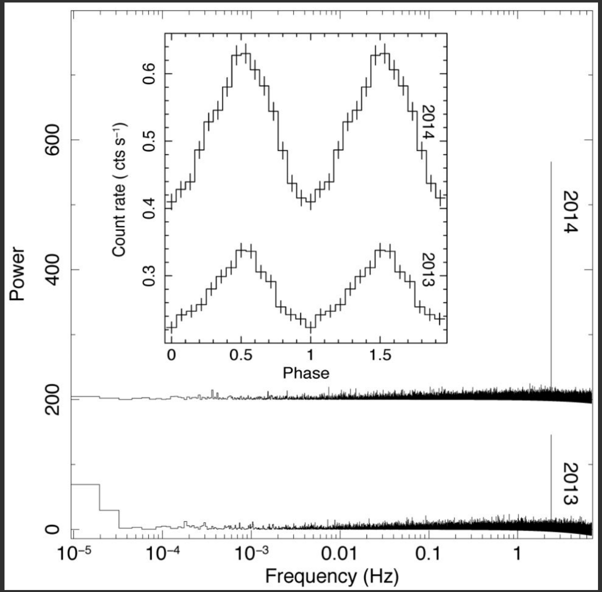

- **Fastest known PULX**:
  - $P_{spin} \simeq 410$ ms
  - $\dot{P}_{sec} \sim -4 \times 10^{-11}$ s s^{-1}
  - $P_{orb} \simeq 65$ d
- **Only PULX with a known optical counterpart** (Motch+ 2014)
- Observed multiple times: Chandra, NICER, NuSTAR, XMM. **Lots of archival data**.
- Long-term monitoring ongoing (see Fuerst+ 2021).

Fuerst+ 2016

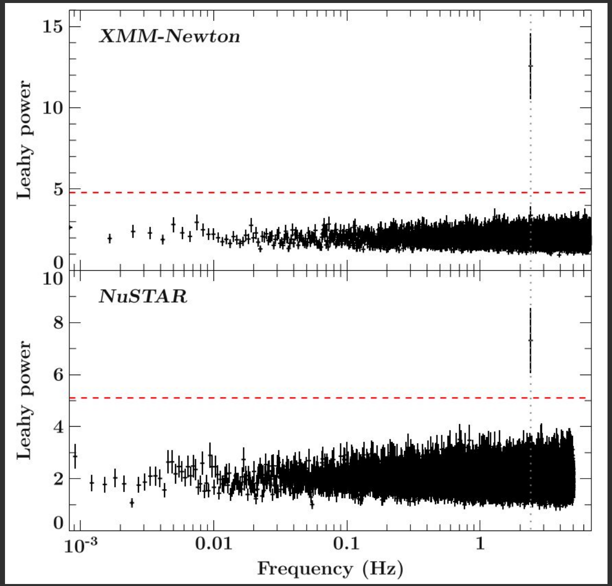

P13: PRELIMINARY RESULTS

PRELIMINARY

- Optical observations with HiPERCAM@GTC and SiFAP2@TNG, quasi-simultaneous with X-ray telescopes: **work in progress**…

- While checking in the X-ray archival data, **we found another QPO**!

- $\nu \simeq 0.01$ Hz.

- Plot above: original PDS, where also the spin signal is visible.

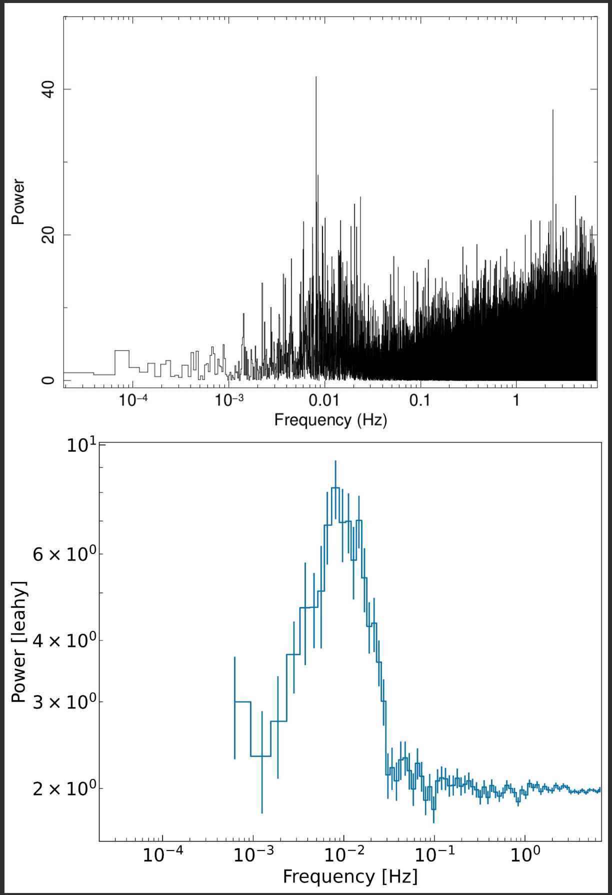

P13: ARCHIVAL DATA

PRELIMINARY

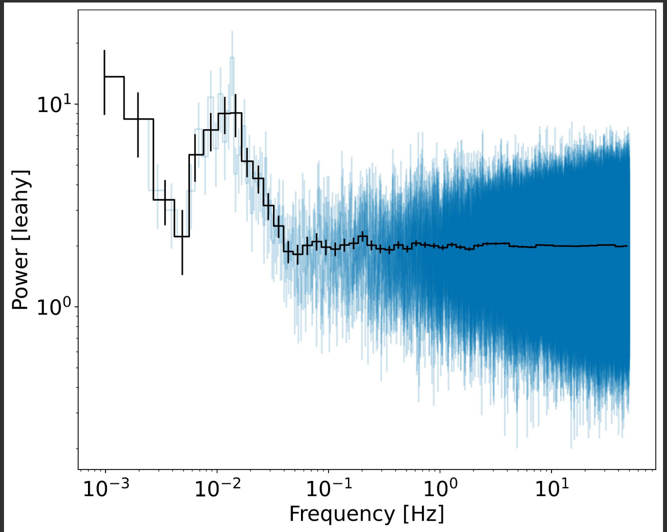

- Detected by different telescopes: NICER, NuSTAR, XMM.

- **When present, always the same frequency**:

  $\nu \simeq 0.01$ Hz

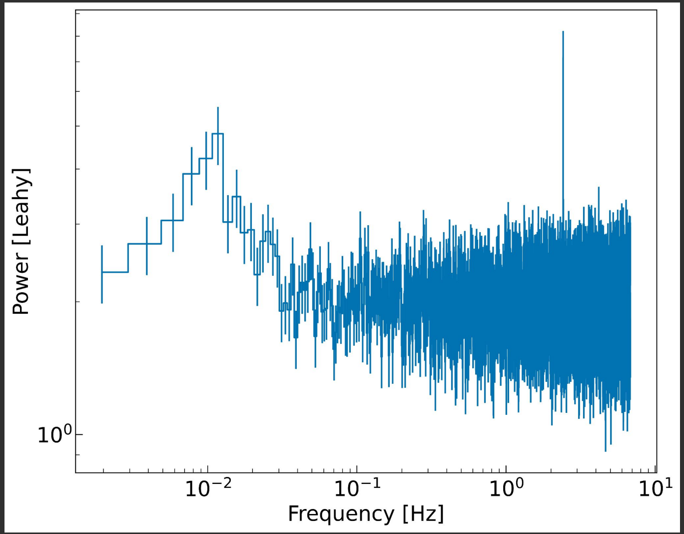

- When both the QPO and the signal are present, the latter has a **very low pulsed fraction**:

  PF ≃ 5-10%

- Typical PF > 20%.

TAKE HOME MESSAGES

- QPOs in the sub-Hz range in ULXs have been widely used as mass-proxy of the accreting compact object: IMBHs candidates.

- M82 X-2 case: **be very careful when constraining the mass of the accretor in the ULX using the QPO frequency!**

- M51 ULX-7: second PULX to show QPO in the mHz-range.
  When present, always detected at the same frequency.
  No signal detected when the QPO is present: **QPO concurrent with a decrease of the pulsed fraction of the signal?**

- If true, the **task of detecting spin signals from a PULX** (a notoriously difficult task) could be **further complicated**.

- **Fraction of PULX over the whole ULX population even higher than previously estimated?**

- QPO in NGC 7793 P13, low PF when present: **common feature among PULXs?**

OPEN TO WORK OFFERS!


SO LONG AND...
Thanks for all the fish!

M51: THE WHIRLPOOL GALAXY

- Pair of interacting galaxies, hosting 9 ULXs (Terashima & Wilson, 2004).
- d ≃ 8.58 Mpc.
- **At least another NS-powered ULX**: M51 ULX-8 (CRSF in the spectrum, no detected pulsation yet; Brightman+ 2018).

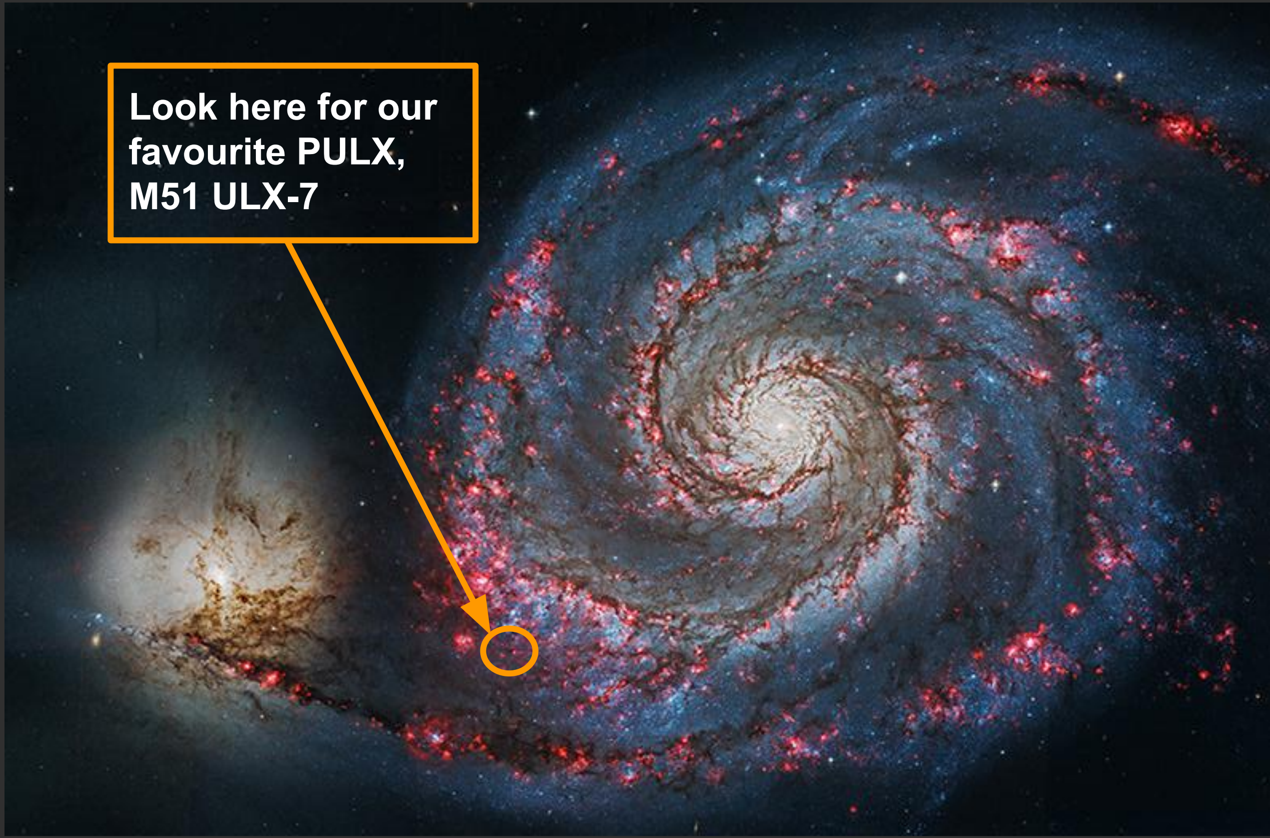

HOW TO DETECT PERIODIC PULSATIONS: POWER SPECTRUM

$$a_j = \sum_{k=0}^{N-1} x_k e^{2\pi i jk/N} \qquad \nu_j = \frac{j}{T}, \nu_{min} = \frac{1}{T}, \nu_{max} = \frac{1}{2\delta t}$$

$$P_j \equiv \frac{2}{N_{\rm ph}} |a_j|^2, N_{\rm ph} = \sum_{k=0}^{N-1} x_k$$

- How do we detect periodic pulsations? Power Spectrum Density (PSD).
- $\boldsymbol{\nu}_j$ = Fourier frequencies.
- Ideal case: white noise (in X we count the number of photons).
- $$\mathrm{Prob}(P_{\rm j,noise} > P_{\rm detect}) = e^{-\frac{P_{\rm detect}}{2}} = \epsilon$$

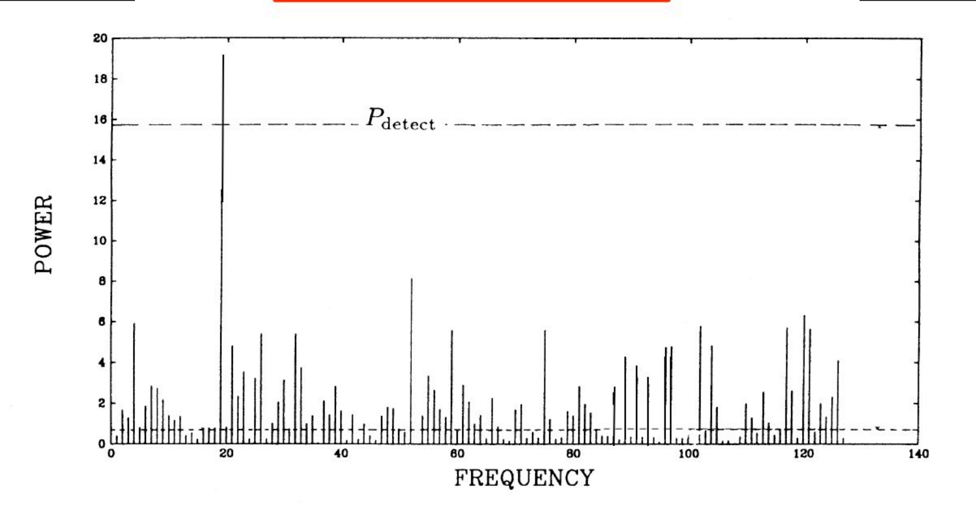

van der Kliis (1988)

A REAL CASE: RED NOISE

- In a real source there are other noise components.
- Red noise: long-term variability.
- $P_j \propto \nu_j^{-\alpha}$
- PSD continuum modeling.

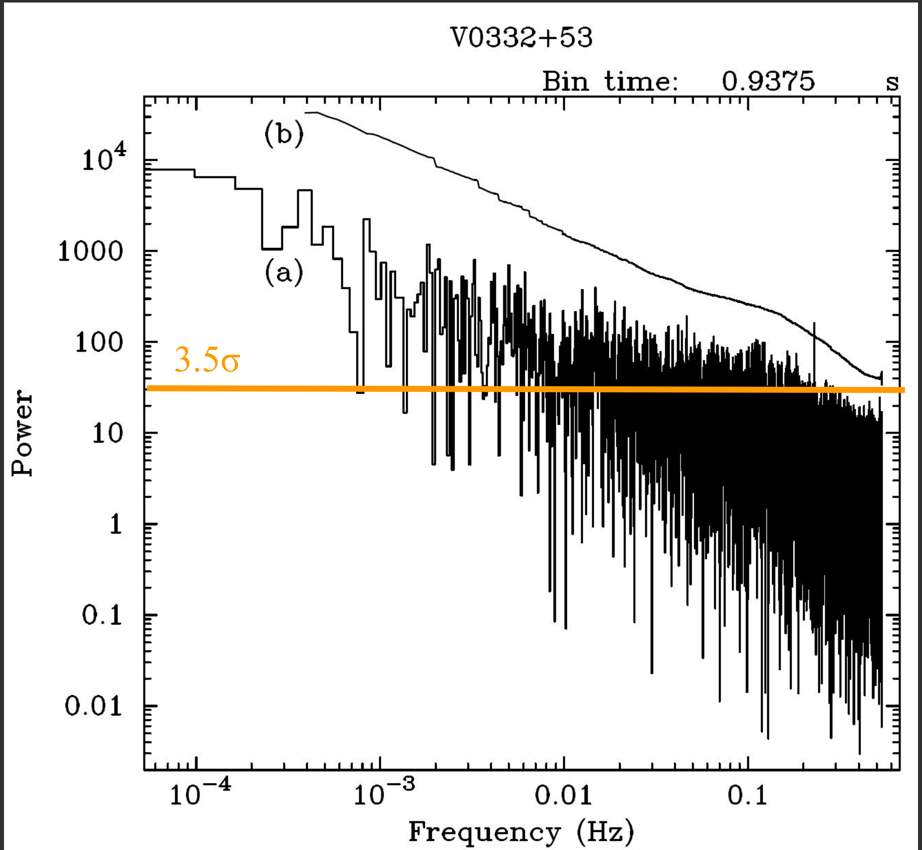

POWER SPECTRUM AND ACCELERATED SEARCH TECHNIQUES

- FFT analysis to detect pulsations.
- $\dot{P} \neq 0$: P varies of $T\dot{P}/P^2$, power **spread over multiple bins**.
- Solution: **accelerated search techniques**.
- Approach: test over various $\dot{P}/P$, searching for optimal correction.

$$t' = t + \frac{1}{2}\frac{\dot{\nu}}{\nu}t^2 = t - \frac{1}{2}\frac{\dot{P}}{P}t^2$$

Case of NGC 5907 ULX-1

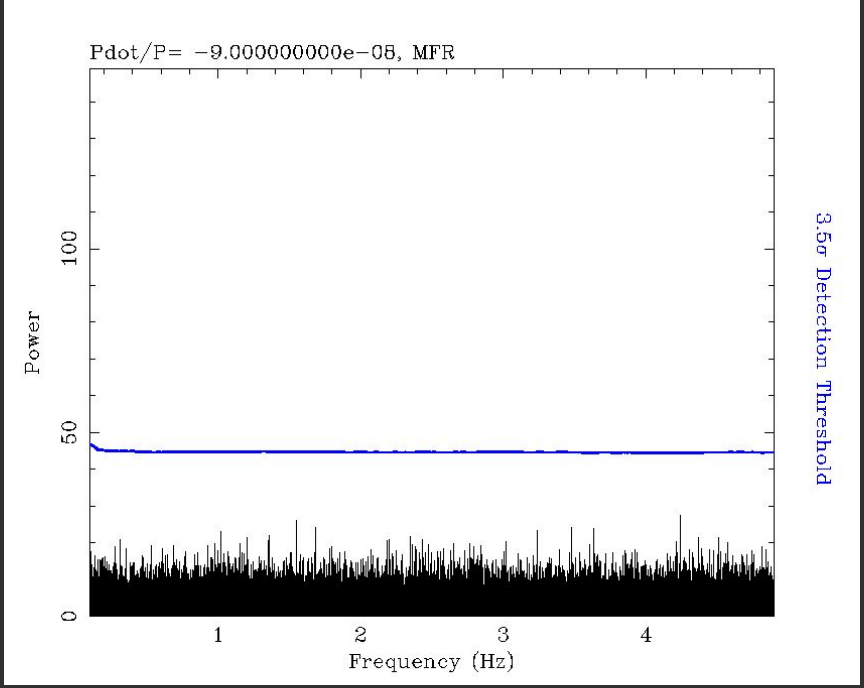

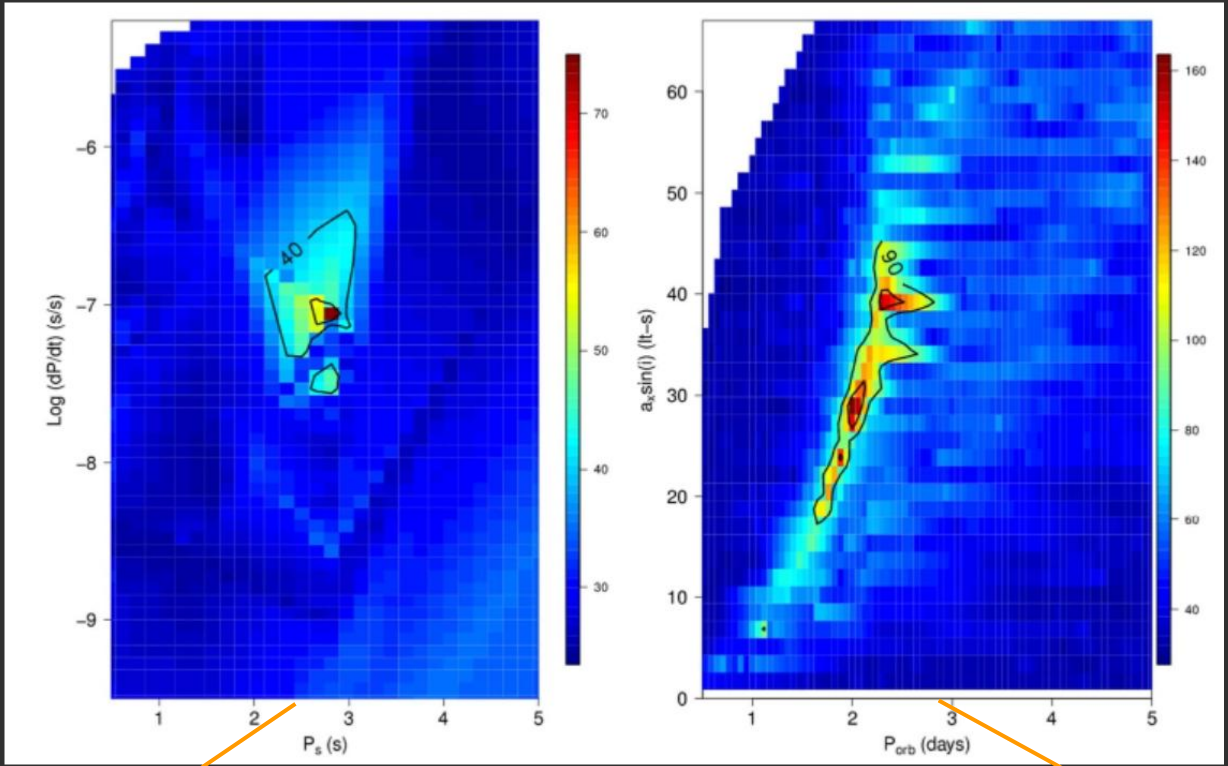

Ṗ/P correction

Orbital motion correction

Table 3. Best-fit spectral parameters of the latest *XMM-Newton* observations with the double-disk model.

Observation	n_H[a] (10^{20} cm^{-2})	kT_{soft} (keV)	Norm.	kT_{hard} (keV)	Norm. (10^{-4})	Flux[b] (10^{-13} erg cm^{-2} s^{-1})	Lum.[c] (10^{39} erg s^{-1})	χ^2/dof	n.h.p.
B	$9.1^{+3.1}_{-2.7}$	$0.32^{+0.04}_{-0.03}$	$0.7^{+0.6}_{-0.3}$	$2.63^{+0.20}_{-0.17}$	$5.7^{+1.5}_{-1.3}$	5.37 ± 0.08	5.34 ± 0.08	297.93/309	0.664
C	$8.1^{+2.5}_{-2.3}$	0.33 ± 0.03	$0.6^{+0.4}_{-0.2}$	$2.78^{+0.21}_{-0.17}$	$4.6^{+1.2}_{-1.0}$	5.37 ± 0.07	5.31 ± 0.07	306.91/337	0.879
B+C	$8.5^{+1.7}_{-1.8}$	0.33 ± 0.02	$0.6^{+0.3}_{-0.2}$	$2.71^{+0.13}_{-0.12}$	$5.0^{+0.9}_{-0.8}$	5.37 ± 0.05	5.33 ± 0.05	607.21/651	0.889

Notes. [(a)] The Galactic absorption component was fixed to $n_{H,gal} = 3.3 \times 10^{20}$ cm^{-2} (HI4PI Collaboration et al. 2016). [(b)] Observed flux in the 0.3–10 keV band. [(c)] Unabsorbed luminosity in the 0.3–10 keV band.

Table 4. Best-fit parameters of the spectra during the peaks and the minima (no-peak) of the modulation of the latest *XMM-Newton* observations. We considered the same double-disk model as before.

Observation	n_H[a] (10^{20} cm^{-2})	kT_{soft} (keV)	Norm.	kT_{hard} (keV)	Norm. (10^{-4})	Flux[b] (10^{-13} erg cm^{-2} s^{-1})	Lum.[c] (10^{39} erg s^{-1})	χ^2/dof	n.h.p.
B									
peak	$10.0^{+5.8}_{-4.7}$	$0.31^{+0.07}_{-0.05}$	$1.1^{+2.0}_{-0.7}$	$2.7^{+0.4}_{-0.3}$	$7.0^{+3.6}_{-2.7}$	7.4 ± 0.2	7.4 ± 0.2	159.28/162	0.546
no-peak	$7.8^{+3.5}_{-3.1}$	$0.34^{+0.05}_{-0.04}$	$0.5^{+0.5}_{-0.3}$	2.8 ± 0.3	$4.0^{+1.7}_{-1.3}$	4.67 ± 0.09	4.61 ± 0.09	288.73/255	0.072
C									
peak	$10.8^{+5.1}_{-4.3}$	$0.30^{+0.05}_{-0.04}$	$1.4^{+1.9}_{-0.8}$	$2.9^{+0.4}_{-0.3}$	$5.7^{+2.8}_{-2.1}$	7.30 ± 0.18	7.46 ± 0.18	175.12/180	0.589
no-peak	$5.8^{+3.0}_{-2.6}$	$0.36^{+0.05}_{-0.04}$	$0.32^{+0.28}_{-0.15}$	$2.8^{+0.3}_{-0.2}$	$4.0^{+1.4}_{-1.1}$	4.62 ± 0.08	4.45 ± 0.08	277.37/277	0.482
B+C									
peak	$10.5^{+3.7}_{-3.2}$	$0.31^{+0.04}_{-0.03}$	$1.3^{+1.2}_{-0.6}$	$2.8^{+0.3}_{-0.2}$	$6.2^{+2.1}_{-1.7}$	7.35 ± 0.13	7.45 ± 0.13	337.69/347	0.63
no-peak	$6.6^{+2.2}_{-2.0}$	$0.35^{+0.04}_{-0.03}$	$0.39^{+0.23}_{-0.14}$	$2.76^{+0.20}_{-0.17}$	$4.0^{+1.0}_{-0.8}$	4.64 ± 0.06	4.52 ± 0.06	567.63/537	0.174

Notes. [(a)] The Galactic absorption component was fixed to $n_{H,gal} = 3.3 \times 10^{20}$ cm^{-2} (HI4PI Collaboration et al. 2016). [(b)] Observed flux in the 0.3–10 keV band. [(c)] Unabsorbed luminosity in the 0.3–10 keV band.

ObsID	$\nu_{\rm QPO}$ (mHz)	$\Delta\nu_{\rm QPO}$ (mHz)	$\nu_{\rm char,QPO}$ (mHz)	$Q_{\rm QPO}$	rms$_{\rm QPO}$ (%)	$\nu_{\rm broad}$ (mHz)	$\Delta\nu_{\rm broad}$ (mHz)	$\nu_{\rm char,broad}$ (mHz)	$Q_{\rm broad}$	rms$_{\rm broad}$ (%)	χ^2/dof
0.3–10 keV											
A	$0.449^{+0.019}_{-0.022}$	$0.088^{+0.054}_{-0.035}$	$0.451^{+0.019}_{-0.022}$	5.1	$29.0^{+3.8}_{-4.0}$	$1.20^{+0.26}_{-0.27}$	$2.60^{+0.67}_{-0.53}$	$1.77^{+0.30}_{-0.27}$	0.5	$37.9^{+2.7}_{-2.6}$	27.74/35
B	$0.470^{+0.012}_{-0.017}$	$0.046^{+0.053}_{-0.046}$	$0.470^{+0.011}_{-0.017}$	10.2	27.4 ± 4.3	$0.92^{+0.18}_{-0.14}$	$1.65^{+0.31}_{-0.26}$	$1.24^{+0.17}_{-0.13}$	0.6	$38.6^{+2.6}_{-2.7}$	24.23/35
C	$0.519^{+0.036}_{-0.033}$	$0.183^{+0.069}_{-0.061}$	$0.527^{+0.036}_{-0.033}$	2.8	32.0 ± 3.6	$1.56^{+0.25}_{-0.23}$	$2.74^{+0.53}_{-0.43}$	$2.08^{+0.26}_{-0.22}$	0.6	40.3 ± 2.6	46.66/37
A+B+C	$0.565^{+0.034}_{-0.036}$	$0.269^{+0.067}_{-0.054}$	$0.581^{+0.034}_{-0.035}$	2.1	29.5 ± 2.4	1.34 ± 0.17	$2.45^{+0.37}_{-0.31}$	$1.81^{+0.18}_{-0.16}$	0.5	36.1 ± 1.8	128.31/124
0.3–1.5 keV											
A[a]	$0.534^{+0.024}_{-0.027}$	$0.148^{+0.062}_{-0.081}$	$0.539^{+0.025}_{-0.028}$	3.6	$32.9^{+3.4}_{-4.0}$	$1.48^{+0.18}_{-0.20}$	$1.56^{+0.76}_{-0.53}$	$1.67^{+0.24}_{-0.22}$	0.9	$32.3^{+2.5}_{-3.4}$	32.26/24
B	$0.467^{+0.014}_{-0.017}$	$0.061^{+0.052}_{-0.035}$	$0.468^{+0.014}_{-0.017}$	7.6	$29.7^{+4.2}_{-4.5}$	$1.04^{+0.40}_{-0.18}$	$1.21^{+0.76}_{-0.48}$	$1.20^{+0.39}_{-0.19}$	0.9	$29.7^{+3.7}_{-3.5}$	43.13/35
C	$0.484^{+0.031}_{-0.028}$	$0.184^{+0.058}_{-0.063}$	$0.493^{+0.031}_{-0.028}$	2.6	$31.8^{+3.5}_{-3.6}$	$1.54^{+0.21}_{-0.24}$	$1.81^{+0.43}_{-0.42}$	$1.79^{+0.21}_{-0.24}$	0.9	33.8 ± 3.2	25.33/35
1.5–10 keV											
A[a]	$0.509^{+0.072}_{-0.044}$	$0.25^{+0.22}_{-0.10}$	$0.525^{+0.075}_{-0.045}$	2.0	$36.9^{+5.1}_{-5.5}$	$1.52^{+0.26}_{-0.43}$	$1.21^{+0.66}_{-0.63}$	$1.64^{+0.27}_{-0.42}$	1.3	$32.7^{+7.6}_{-6.3}$	34.30/23
B	$0.469^{+0.014}_{-0.022}$	$0.047^{+0.067}_{-0.047}$	$0.470^{+0.014}_{-0.022}$	9.9	25.8 ± 5.3	$1.03^{+0.19}_{-0.18}$	$1.68^{+0.38}_{-0.31}$	$1.33^{+0.19}_{-0.17}$	0.6	$46.3^{+3.8}_{-3.3}$	22.67/35
C	$0.538^{+0.028}_{-0.041}$	$0.26^{+0.12}_{-0.10}$	$0.553^{+0.030}_{-0.042}$	2.1	34.6 ± 5.4	$1.27^{+0.71}_{-0.53}$	$4.08^{+0.98}_{-0.81}$	$2.40^{+0.55}_{-0.44}$	0.3	$47.5^{+3.9}_{-4.9}$	34.71/35

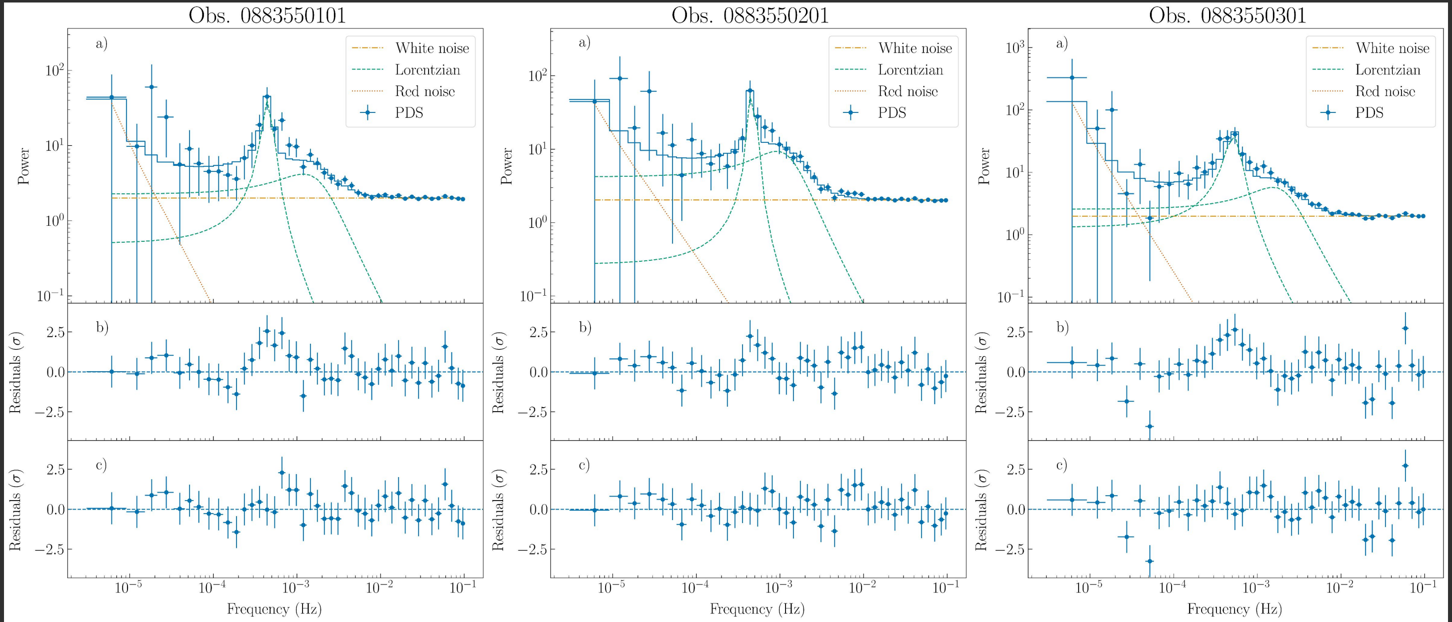

Obs. 0883550101
Obs. 0883550201
Obs. 0883550301
a)
b)
c)
White noise
Lorentzian
Red noise
PDS
Power
Residuals (σ)
Frequency (Hz)

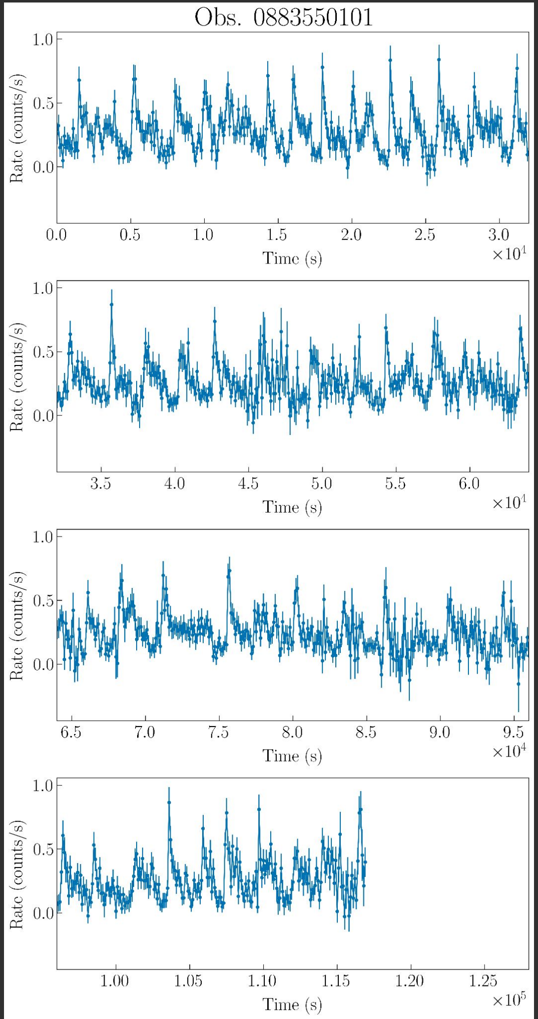
Obs. 0883550101
Rate (counts/s)
Time (s)

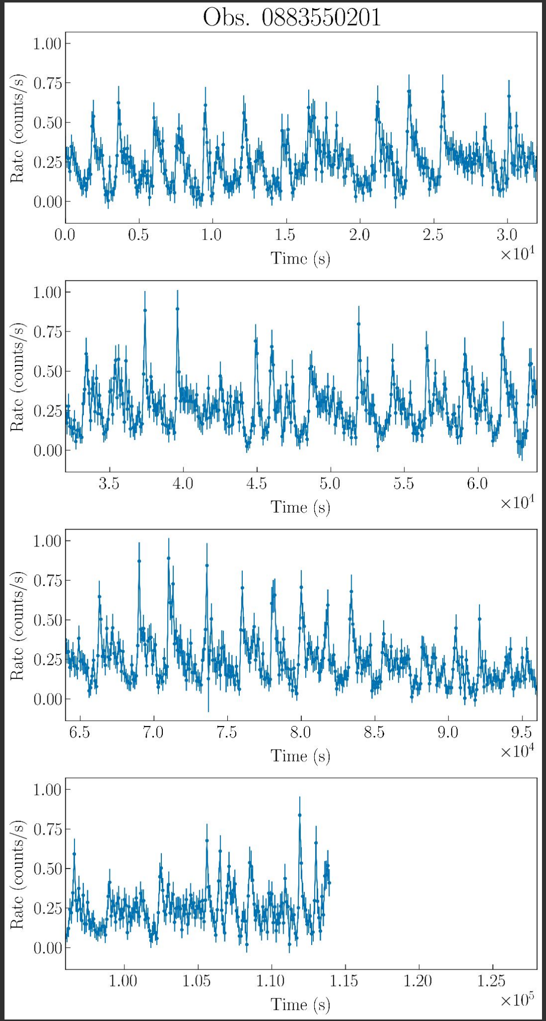
Obs. 0883550201
Rate (counts/s)
Time (s)

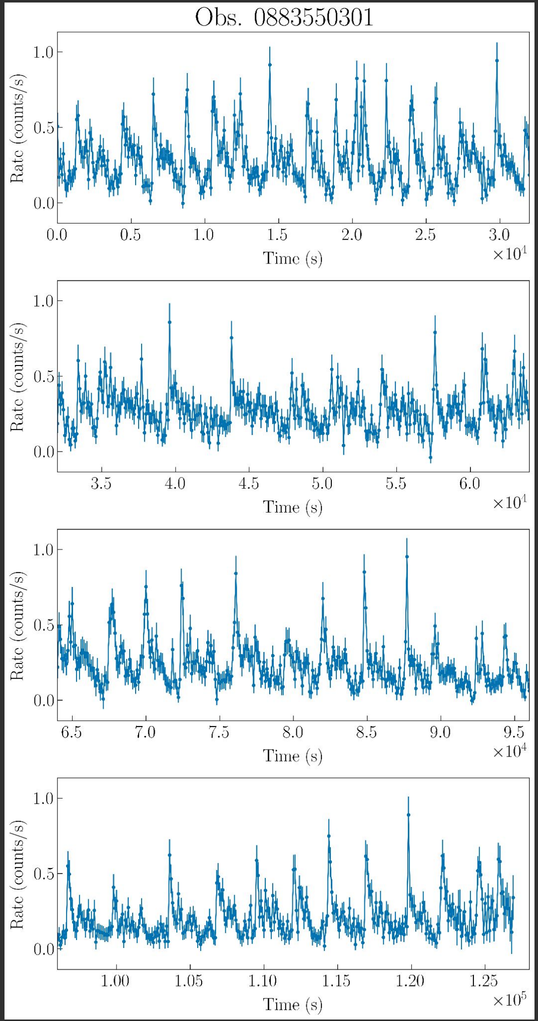
Obs. 0883550301
Rate (counts/s)
Time (s)

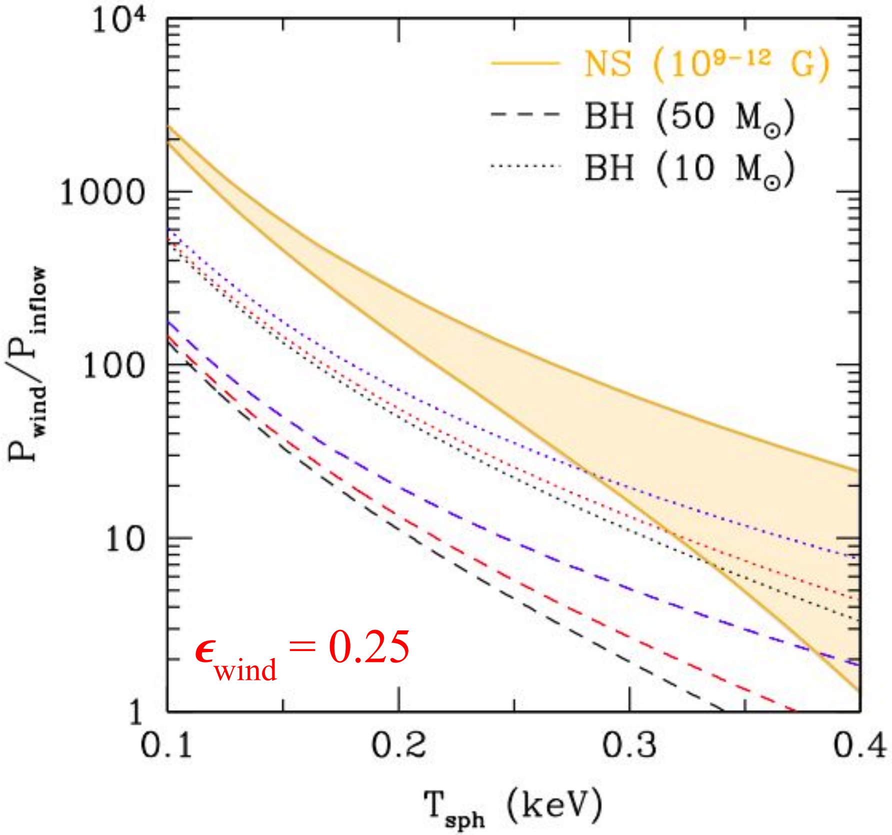

10^4
1000
100
10
1
0.1
0.2
0.3
0.4
P_{wind}/P_{inflow}
T_{sph} (keV)
NS (10^{9-12} G)
BH (50 $M_\odot$)
BH (10 $M_\odot$)
$\epsilon_{wind} = 0.25$

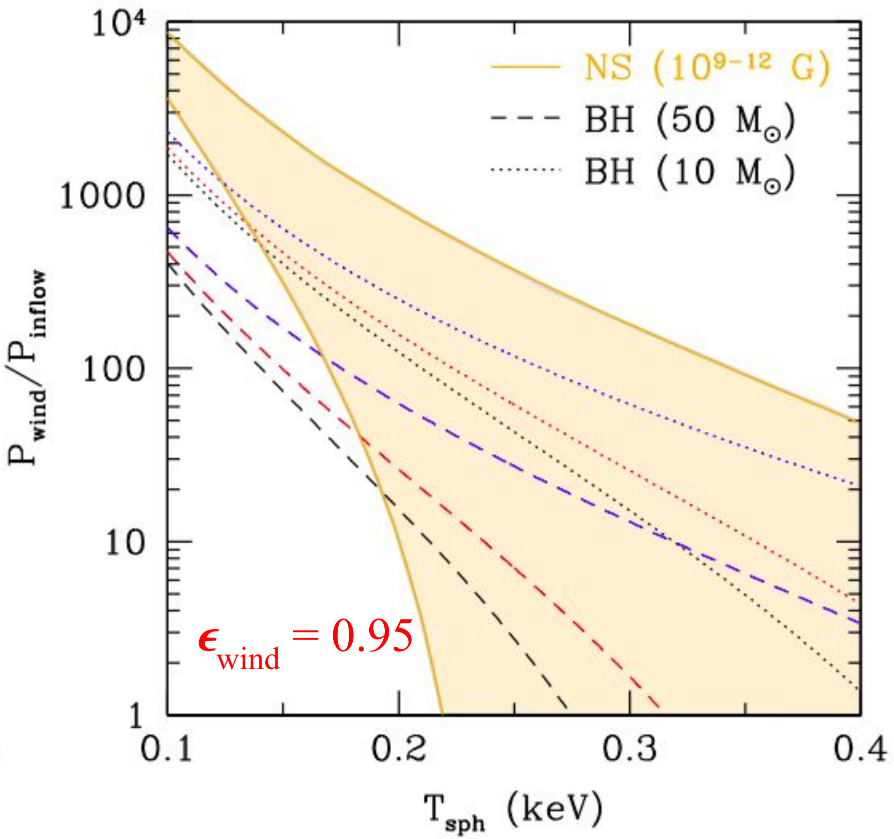

10^4
1000
100
10
1
0.1
0.2
0.3
0.4
P_{wind}/P_{inflow}
T_{sph} (keV)
NS (10^{9-12} G)
BH (50 $M_\odot$)
BH (10 $M_\odot$)
$\epsilon_{wind} = 0.95$